ADDIS ABABA UNIVERSITY
SCHOOL OF GRADUATE STUDIES
DEPARTMENT OF CHEMISTRY

Stripping square wave voltammetry for the determination of uric acid in human urine using Fe^{3+} doped zeolite graphite powder composite modified glassy carbon electrode.

A Thesis presented to the School of Graduate Studies Addis Ababa University in partial fulfillment of the requirements for the degree of Master of Science in Chemistry.

By: Tadesse G/giyorgis

Asvisors: Dr. Merid Tessema
Dr. Shimelis Admassie

June, 2011

Acknowledgement

I would like to express my deepest gratitude to my advisors Dr. Merid Tessema and Dr. Shimelis Admassie for their valuable guidance, consistence encouragement and constructive criticism throughout my thesis work and I would like to thank again Dr. Shimelis with deepest gratitude for willing to work in his laboratory as a result of which I was free to use all the required materials available in the laboratory.

My sincere gratitude goes to Professor Isabel Diaz for giving me the zeolite Y chemical that is not available in the chemical store.

Finally I would like to thank Addis Ababa University for sponsoring my education, Ato Maereg Amare (PhD. Student at department of chemistry, AAU) for the support of the sample for this thesis work and AAU department of chemistry for providing me with laboratory and other facilities for this work to accomplish.

Contents

List of figures

List of abbreviation

ZME	zeolite modified electrode
UA	uric acid
$Fe^{3+}Y$/GPC	iron (III) doped zeolte graphite powder composite
GCE	glassy carbon electrode
GPMGCE	graphite powder modified glassy carbon electrode
PBS	phosphate buffer solution
GPC	graphite powder composite

Abstract

A novel stripping square wave voltammetric method has been developed for the determination of uric acid (UA) in untreated human urine using iron (III) doped zeolite/graphite powder composite modified GCE. The synergetic effects of the catalytic role of Fe^{3+}, larger surface area of zeolite, and higher conductivity of graphite powder account for the anodic peak current obtained at much lower positive oxidation potential than at the bare GCE. The proposed method is simple, rapid, has excellent selectivity, reproducible and sensitive in the linear range of 2–80 μM UA with a detection limit of 2.3×10^{-7} mol L^{-1}. The developed method enabled to achieve recoveries ranging from 90.98 to 106.77% of spiked standard UA from untreated human urine with a standard error of less than unity.

Key words: Zeolite NaY (zeolite), Iron doped zeolite, undoped zeolite, stripping SWV, chemically modified electrode (CME), uric acid (UA), human urine, polystyrene, dichloroethane, tetrahydrofuran (THF)

1. Introduction

1.1. Uric acid

Uric acid (UA) is the primary final-product of purine metabolism, which is largely removed by the kidneys. The concentration of UA in serum is approximately 240 – 520 mM with urinary excretion in the range 250-750 mg/L over a 24 hour period for a healthy individual [1]. Abnormal levels of UA in urine and serum indicate symptoms of several diseases namely gout, hyperuricemia, pneumonia and Lesch –Nyhan syndrome. Therefore the detection and quantification of uric acid in human physiological fluids is important for the diagnosis of patients suffering from a range of disorders associated with altered purine metabolism.

1.2. Properties of Uric acid

Uric acid is aromatic because of the purine functional group. Uric acid has a molecular formula $C_5H_4N_4O_3$ and a molecular mass of 168 g/mol, It is white crystalline in appearance, slightly soluble in water and has a density of 1.87 g/mL [2].

Uric acid is a diprotic acid with pKa_1=5.4 and pKa_2=10.3. Thus in strong alkali, it forms the dually charged full urate ion, but at biological pH or in the presence of carbonic acid or carbonate ions, it forms the singly charged hydrogen or acid urate ion as its pKa_2 is greater than the pKa_1 of carbonic acid. As its second ionization is so weak, the full urate salts tend to hydrolyze back to hydrogen urate salts and free base at around neutral pH values.

1.3. Determination of Uric acid

The development of a simple and rapid methodology for the determination of UA has attracted attention in recent years [3– 6]. A range of techniques which include chromatography, [7 – 11] electrophoresis, [12, 13] mass spectroscopy, [14] enzymatic and colorimetric methods [15, 16] have been reported and widely used for qualitative and quantitative detection of uric acid. These analyses are generally performed at centralized laboratories, requiring extensive labor and

analytical resources, and often result in a lengthy turn-around time. Electrochemical methods offer an analytical platform which can exhibit a higher selectivity and sensitivity than the other commonly employed methods and have the inherent advantage of lower cost and rapid sensing time.

Recently electrochemical sensors and biosensors attracted considerable interests because of their high sensitivity, low instrumentation costs, a ready capacity for miniaturization, and direct electronic readout [17-19]. Electrochemical detection of UA can provide inexpensive and rapid screening techniques and support conventional techniques for both laboratory and field analysis. Various electrochemical sensors and biosensors, such as Nafion-coated carbon paste electrode[17], Poly(N,N-dimethylaniline) film-coated GC electrode [18], Glassy carbon electrode coated with paste of multiwalled carbon nanotubes and ionic liquids [19], Cysteine modified glassy carbon electrode [20], Carbon-coated iron nanoparticle modified glassy carbon electrode [21], Iron(III) doped zeolite modified carbon paste electrode [22], poly(bromocresol purple) modified glassy carbon electrode [23] and so on, have been developed for the sensitive determination of UA.

The official method for the determination of uric acid in clinical laboratory is using spectrophotometer. Uric acid is oxidized by uricase to produce allantoin and hydrogen peroxide. The hydrogen peroxide reacts with 4-aminoantipyrine and 3,5-dichloro-2-hydroxybenzene sulfonate in a reaction catalyzed by peroxidase to produce a colored product. The change in absorbance is directly proportional to the concentration of uric acid in the sample.

In our present investigation, iron (III) doped zeolite/graphite powder composite (Fe^{3+}Y/GPC) modified GCE was prepared. The electrochemical characteristic of the modified electrode were studied and was used for the determination of uric acid in urine.

1.4. Zeolite

Zeolites are hydrated crystalline aluminosilicate minerals, natural or synthetic, with the general formulation $(C^{n+})_x[(AlO^-_2)_{nx}(SiO_2)_y].m(H_2O)$ and are widely used as adsorbents, ion exchangers, or catalysts.

The zeolite structure is based on a three-dimensional network of Al- or Si-centred tetrahedra which are linked to each other via doubly bridging oxygen atoms. This continuous three-dimensional pattern forms a system of cages and channels of defined dimensions with minimum and maximum diameters, conferring to the zeolites unique molecular sieving properties applied to both shape and size molecular discrimination. The presence of aluminium in the framework induces an excess negative charge, requiring the introduction of charge-compensating cations (C^{n+}) into the structure. These extra-framework cations are not covalently bound to the zeolite structure; they have considerable freedom of movement and can be readily substituted with a variety of other cations, conferring ion exchange properties to these aluminosilicates. Many electroactive cations have been incorporated into zeolites and their charge-transfer reactions have been studied using electrochemistry or spectroscopic techniques [24, 25].

1.5. Electrochemistry involving zeolites

The first report using zeolites for electrochemical purposes, dated 1939, has been described by Marshall and involves the potentiometric response of zeolite-containing membrane electrodes to various mono- and divalent cations [26]. This work and some subsequent investigations by the same group considered the inorganic membranes as polyelectrolytes with mobile cations, allowing the characterization of cation activities similar to the way that the glass membrane electrode is used for determining hydrogen ion activities. This pioneering approach was then pursued by Barrer and James [27] in 1960, providing a more quantitative treatment of the zeolite membrane potential and discussing its relation to the selectivity with respect to cation mixtures in solution. Such potentiometric applications exploit the solution-like ionic conduction of zeolites. A few years later, the solid-state ionic conduction of zeolites was utilized in

electrochemistry by designing solid-state batteries [28] and fuel cells, with zeolite particles acting as a solid electrolyte and as a host for the catholite (in batteries) or for electroreactants or water (in fuel cells). Finally, at the end of the 1970s, Susic and Petranovic investigated the electrochemical behavior of dry zeolite crystals at temperature above 200°C, where dry zeolite displays solid-state ionic conduction. At these high temperatures, the zeolite acted as a ‘’solvent’’ for the charge-compensating cations that can be reduced on platinum; examples are available for reduction of Na^+, Cd^{2+}, and Ag^+ [29]. These latter investigations are the first examples of electrodics involving zeolites, while the above potentiometric experiments were only concerned with ionics.

Modern fields of investigation concerning the zeolite-electrochemistry intersection began in the 1980s with considerable research on ZMEs since 1988. It is noteworthy that the (often) preliminary works performed in this initial mid 80’s period suggested most of the application types as well as electrode configurations. Some milestones are:

Pereira-Ramos et al. [30] prepared zeolite-supported metal catalyst using electrochemical techniques. By means of a pressed composite electrode made of graphite and silver-exchange mordenite particles, they were able to produce electrochemically some clusters of metallic silver within the mordenite particles, and crystallities or dendritic deposits on the graphite particles. One year later, Murray et al. [31] grew electrogenerated coatings comprising zeolites; this was achieved by continuous potential cycling at a rotated disk electrode (Pt or C) in an organic solvent containing fine zeolite particles in suspension and an appropriate soluble electroreactant. Concurrent and competing with this approach is the evaporative deposition of a zeolite-polystyrene composite layer on solid electrode surfaces, which is carried out with suspensions of powdered zeolite in polymer solutions, as first described by de Vismes et al. [32]. They have also incorporated some metal porphyrins into the ZME and explored their electrocatalytic properties; in this case, the zeolite is thought to enhance the chemical stability of the catalyst.

Hernandez et al. [33] described the first zeolite-modified carbon paste electrode, by mixing graphite particles with a natural zeolite from the Canary Island and a mineral oil binder, they applied it to the voltammetric analysis of Hg^{II} after chemical accumulation by ion exchange within the zeolite.

Finally, the group of Shaw [34] initiated what has become one of the largest challenges of ZME electrochemistry: (a) to determine and, if possible, control the factors affecting the behavior of ZMEs; and (b) to understand the origin of the electrochemical response of ZMEs by proposing mechanistic models for charge transfer.

At the end of the 1980s, the two main methods for preparing ZMEs were zeolite overlayers on solid electrodes and zeolite dispersions into a composite electrode material. Subsequent efforts were often directed to optimizing these generic procedures to get longer durability and better electrochemical perspectives, rather than evaluating totally new directions (e.g., in situ grown zeolite films on conducting substrates like gold or mercury [35]. The main applications predicted during this startup period, including electrocatalysis and several aspects of electroanalysis and sensors, were largely developed during the last decade of the 20th century. One should also mention that the field of energy storage that exploits the adsorbent properties of zeolites was still growing in the 1980s, especially prompted by Coetzer [36], and the use of zeolites as solid electrolytes in batteries remains common.

1.6. **Design and preparation of zeolite modified electrodes**

Starting an electrochemical study with electronically insulating zeolite particles implies confining them at an electrode surface. This construction step should be reasonably easy and should provide ZMEs with good conductivity properties (low resistance and low capacitance), high mechanical stability and long-term durability, as well as reproducible characteristics (both for their fabrication procedures and their electrochemical responses). Of course, such ideal conditions leading to high-quality chemically modified electrodes that would display adequate electrochemical signals are not easily fulfilled when zeolite is used as the electrode modifier. This is because its insulating character will lower the electrode conductivity, and individual solid crystals of micrometer dimension and rigid structure will result in heterogeneous composition and configuration of the modified electrode material. This in turn could impart rather low mechanical stability in stirred media due to possible leaching of zeolite particles into the solution. These are some of the reasons why many efforts have been directed to finding the best strategies to prepare ZMEs.

A classical route to chemically modify an electrode surface is to cover it with an adhesive layer of the modifying agent. This simple approach was successfully applied to polymer modified electrodes, but it is prevented here as the zeolite particles do not stick by themselves to the surface of conventional electrodes. Cohesion would require a binder. This is what has motivated the development of zeolite-polymer film coated on solid electrode surfaces.

Composite zeolite-polymer film can be easily deposited on a solid electrode by evaporation of an organic solution containing a dissolved polymer (mainly polystyrene) and suspended zeolite particles. This rather simple procedure has been widely used [34] and gives rise to porous films that enable the diffusion process to occur at the electrode-film-solution interfaces by way of the free space (‘’void’’) remaining in the composite after solvent evaporation

Another way to improve the conductivity of ZMEs made of two resistive elements (i.e., polystyrene and zeolite) is to add carbon powder to the film. This is readily achieved by grinding together carbon and zeolite particles prior to dispersing them in the polymeric binder [37]. If resistance of these films was indeed lowered as compared with that of carbon-free coatings, it should be emphasized that capacitance of the ZME was also significantly increased due to a much higher area of the electrode surface.

The most widely used method to prepare ZMEs is the incorporation of zeolite particles into the bulk of a so-called carbon paste. Carbon paste was invented a long time ago and consists of a homogeneous mixture of carbon powder and pasting liquid [38]. This matrix has taken a prominent position in the development of chemically modified electrodes because of its good electrochemical characteristics and its simple modification by a large variety of chemicals and biochemicals [39]. It is therefore not surprising that many investigations on ZMEs were carried out using zeolite-modified carbon paste electrodes (ZMCPEs) [40]. Their surfaces can be renewed by simple mechanical smoothing, which constitutes a definite advantage over film-based ZMEs that would require the fabrication of a new electrode between each measurement (at least if chemical regeneration cannot be applied). However, the high reproducibility of the mechanical renewing of ZMCPE requires a homogeneous composition of the zeolite-modified paste (not so easily obtained).

1.7. Electron transfer mechanisms in ZMEs

The two main requirements for an electroactive probe ion exchanged or encapsulated in a zeolite network to undergo a charge transfer reaction are the following:

a. The electroactive species must be connected to a conductive electrode material (either in physical contact to the electrode, close enough to experience direct electron transfer, or mobile enough to freely diffuse to the electrode surface); alternatively, the electroactive species can undergo indirect charge transfer by way of either a suitable mediator that can act as a relay between the electrode and the probe (electrocatalysis) or a sufficiently high density population of the electroactive probes that allows self-exchange of electrons between them (electron hopping) [40];
b. Charge balance must be maintained in the zeolite ; therefore, the overall charge-transfer reaction is inevitably associated with a mass transport process: at any time the amount of fixed negative charges in the zeolite network must be counterbalanced by an equivalent amount of cation, so that any reduction of a cationic probe initially exchanged in the zeolite would require the ingress of another cationic species in the bulk material; similar charge compensation would be achieved by cation expulsion from the zeolite upon oxidation of the electroactive probe [41].

This interplay between charge transfer and mass transport is at the origin of the mechanisms proposed in the literature to explain the electrochemical behavior of ZMEs, and underscores the key role played by diffusion of both electroactive probes and electrolyte cations in affecting the voltammetric responses.

According to the original model of Shaw and coworkers [41] and subsequent amendment by Dutta and Ledney [42], three distinct pathways for describing charge-transfer reactions occurring at ZMEs can be operative. Beside the purely intrazeolitic [Eq. (1) or extrazeolitic [Eqs. (2a) and (2b)] electron transfer processes, the concept of surface-mediated charge transfer [Eqs. (3)- (5)] was introduced by distinguishing between bulk- and surface-located ion-exchange sites.

Mechanism I:

$$E_{(z)}^{m+} + ne^- + nC_{(s)}^+ \text{ <=> } E_{(z)}^{(m-n)+} + nC_{(z)}^+ \quad (1)$$

Mechanism II:

$$E_{(z)}^{m+} + nC_{(s)}^+ \text{ <=> } E_{(s)}^{m+} + nC_{(z)}^+ \quad (2a)$$

$$E_{(s)}^{m+} + ne^- \text{ <=> } E_{(s)}^{(m-n)+} \quad (2b)$$

Mechanism III:

$$E_{(z,surf)}^{m+} + ne^- + nC_{(s)}^+ \text{ <=> } E_{(z,surf)}^{(m-n)+} + nC_{(z,surf)}^+ \quad (3a)$$

$$E_{(z,surf)}^{(m-n)+} + nC_{(z,surf)}^+ + E_{(z,bulk)}^{m+} \text{ <=> } E_{(z,bulk)}^{(m-n)+} + nC_{(z,bulk)}^+ + E_{(z,surf)}^{m+} \quad (3b)$$

$$M_{(s)}^{m+} + ne^- \text{ <=> } M_{(s)}^{(m-n)+} \quad (4a)$$

$$M_{(s)}^{(m-n)+} + nC_{(s)}^+ + E_{(z,surf)}^{m+} \text{ <=> } E_{(z,surf)}^{(m-n)+} + nC_{(z,surf)}^+ + M_{(s)}^{m+} \quad (4b)$$

$$M_{(z,surf)}^{m+} + ne^- + nC_{(s)}^+ \text{ <=> } M_{(z,surf)}^{(m-n)+} + nC_{(z,surf)}^+ \quad (5a)$$

$$M_{(z,surf)}^{(m-n)+} + nC_{(z,surf)}^+ + E_{(z,bulk)}^{m+} \text{ <=> } E_{(z,bulk)}^{(m-n)+} + nC_{(z,bulk)}^+ + M_{(z,surf)}^{m+} \quad (5b)$$

Where E is the electroactive species with charge m^+, C^+ represents the electrolyte cation (chosen as monovalent for convenience), M is a mediator (chosen with charge m^+ for convenience), the subscript z and s refer to the zeolite phase and the solution, respectively, and the subscripts surf and bulk refer to the zeolite surface (either external surface or outermost subsurface layer of cages) and bulk ion-exchange sites.

Mechanism I is purely intrazeolitic, where the electroactive species undergoes intracrystalline electron transfer while charge balance is maintained by solution phase electrolyte cations entering the zeolite framework [Eq. (1)]. It is to be noted that this mechanism does not distinguish between species located deep in the bulk zeolite and those situated in the boundary region of the zeolite grains. Mechanism II is purely extrazeolitic and involves the ion-exchange

of the electroactive probes for the electrolyte cations [Eq. (2a)] prior to their electrochemical transformation in the solution phase [Eq. (2b)]. The group of mechanism III distinguishes between the electroactive probes located in the bulk zeolite and those situated at the external boundary of the particle. The first case is the direct electron transfer to electroactive species situated at the outer surface of the zeolite particles (i.e., those easily accessible to the electrons), with charge compensation ensured by the electrolyte cation [Eq. (3a)]. This step can be (but is not necessarily) followed by electron hopping to the probes located in the bulk of the solid, with concomitant migration of the electrolyte cation inside the zeolite structure [Eq. (3b)]. In the presence of charge-transfer mediator either dissolved in solution or adsorbed on the zeolite surface, electrochemical transformation [Eqs. (4a) and (5a)] can lead to indirect charge transfer to either surface-confined or bulk-located electroactive probes [Eqs. (4b) and (5b)]. Although some unambiguous evidence is available to support one or another of these mechanisms, all of these theoretical pathways have yet to be demonstrated at practical levels.

More versatility can be added to these mechanistic pathways by defining topological regions of a zeolite as experienced by an electrochemical probe molecule. This concept was introduced by Bessel and Rolison [43], according to a terminology that was previously specified for photoelectron transfer reactions in zeolites. Four topological redox isomers can be designated: (a) the solution phase redox solute originating from the zeolite interior; (b) the electroactive probes located at the zeolite boundary (either adsorbed on the outer surface or occluded in defect sites, or even encapsulated in the outermost layer of the zeolite particle); (c) the redox probes situated in the bulk zeolite but free to experience the global pore lattice over the time scale of the experiment; and (d) the electroactive solutes strictly confined in the zeolite interior by physical entrapment preventing them from motion from one site to another. In the various mechanisms described by Eqs. (1)-(5), the first species are assigned as ‘’S’’ (solution phase), the second as ‘’surf’’ (zeolite surface boundary), and the third and fourth as ‘’bulk’’ (zeolite interior).

Based on the electrochemical behaviors described above and others from the literature a briefly summarized (and consequently restricted) view of the actual situation dealing with electron transfer mechanisms at ZMEs, is the distinction between two categories of solutes in zeolite [25]:

a. Ion-exchangeable electroactive probes that are mobile in the zeolite lattice and can therefore be subjected to ion exchange with the electrolyte cations, These undergo extracrystalline electron transfer according to mechanism II [Eqs. (2a) and (2b)]. Several experiments indicate that a chemical ion-exchange step occurs prior to traditional electrochemical transformation of the probe at the electrode solution interface [44]. While intrazeolite electron transfer was suggested for non-size-excludedredox probes [45], no unequivocal demonstration was provided for this, except when using appropriate spatially arranged mediators [Eqs. (4) and (5)] [46]. Note that intrazeolite mass transport processes (i.e., site-to-site diffusion from small to large cages) may influence extracrystalline electron transfer.

b. Encapsulated complexes that are physically trapped in the zeolite pore structure and are therefore experiencing high steric constraints, These are amenable to electron transfer if located in the boundary region of the zeolite grains. An important question is the exact nature of these species situated in the outermost layers of the zeolite grains, which are considered either as extrazeolitic [Eq. (3a)] or intrazeolitic [Eq. (1)] according to the authors [47]. This leads to a large amount of electrochemically silent species (those located in the bulk zeolite, i.e., 98-99%), which can be slightly but not dramatically improved by the use of adsorbed mediators [Eqs. (5a) and (5b)].

2. Electroanalytical technique

Voltammetry is a versatile technique for research purposes. It allows the research into several aspects of electrochemical reactions, namely those reactions in which electrons are exchanged between reagents and products. For such reaction it is possible to investigate the dependence of the current on the potential when an electrode is dipped into the reaction environment in which they take place [48].

Voltammetry is an electroanalytical technique based on the measurement of current flowing through an electrode dipped in solution containing an electro active compounds while a potential

is imposed upon it [49, 50]. Voltammetry is typically performed using a three electrode potentiostat, which accurately controls the applied potential. The redox reaction takes places at the working electrode, because the working electrode is where the reaction or transfer of interest is taking place. This electrode could be composed of several materials. Usually, it has a very little surface in order to assume quickly and accurately the potential imposed by the electrical circuit. The electrode can be solid (platinum, gold or glassy carbon) formed by a drop of mercury hanging from tip of capillary. If the electrode is formed by a drops of mercury rhythmically dropping from a capillary, the analytical technique is called polarogaphy [48]. The second electrode is a reference electrode, which maintains a constant potential throughout the experiments, and the third electrode the counter electrode, which complete the electrical circuit. The counter electrode also known as the auxiliary electrode, is often much larger than working electrode to minimize current density at the electrode surface [50].

The common characteristic of all voltammetric techniques is that they involve the application of a potential (E) to an electrode and the monitoring of the resulting current (i) flowing through the electrochemical cell [47]. In many cases the applied potential is varied or the current is monitored over a period of time (t). Thus, all voltammetric techniques can be described as some function of E, i, and t. They are considered active techniques (as opposed to passive techniques such as potentiometry) because the applied potential forces a change in the concentration of an electroactive species at the electrode surface by electrochemically reducing or oxidizing it.

The analytical advantage of various voltammetric techniques include excellent sensitivity with very large useful linear concentration range for both inorganic and organic species (10^{-12} to 10^{-1} M), a large number of useful solvents and electrolytes, a wide range of temperature they allow, rapid analysis times (seconds) simultaneous determination of analytes, the ability to determine kinetics and mechanistic parameters, a well developed theory and thus the ability to reasonably estimate the values of unknown parameters, and the case with which different potential wave-forms can be generated and small current measured.

The use of the voltametric techniques is the basis of the comprehension of the laws concerning several electrochemical phenomena and has a great importance in several technological fields like: research of corrosion-proof materials (corrosion is a consequences of a series of

electrochemical reactions), research of new electrodic process for chemical industries (in fact for example, millions of tons of aluminum, chlorine, soda are produced by means of electrochemical reactions) and the production of new type of batteries that can store rapidly high quantity of energy. It is also used in quantitative analysis of trace of metals those of oxidazable or reducible chemicals at ug/L levels or less [48].

2.1. Cyclic voltammetry

Cyclic voltammetry is the most effective and versatile electro analytical technique for the study of electro active species. Its versatility was combined with ease of the measurement and has resulted in extensive use cyclic voltammetry in the field of electrochemistry, inorganic chemistry, organic chemistry and biochemistry. The effectiveness of cyclic voltammetry results from its capability for rapid observing redox behavior over a wide potential range [56]. It was the most widely used technique of all methods by both electrochemist and non electrochemist alike. It allows the analyst to mechanistically study systems, especially the assignment and characterization of redox couples [49].

Cyclic voltammetry consists of cycling the potential of an electrode, which is immersed in unstirred solution and measuring the resulting current. The potential of the working electrode is controlled verses a reference electrode such as saturated calomel electrode (SCE) ($Hg/Hg_2Cl_2/Cl^-$) or $Ag/AgCl/Cl^-$. The controlling potential that is applied across these two electrodes can be considered an excitation signal. The excitation signal for cyclic voltammetry is linear potential scan with a triangular wave–form as shown in figure (1). This triangular potential excitation signal sweeps the potential of the electrode between two potentials sometimes called the switching potential [50, 51].

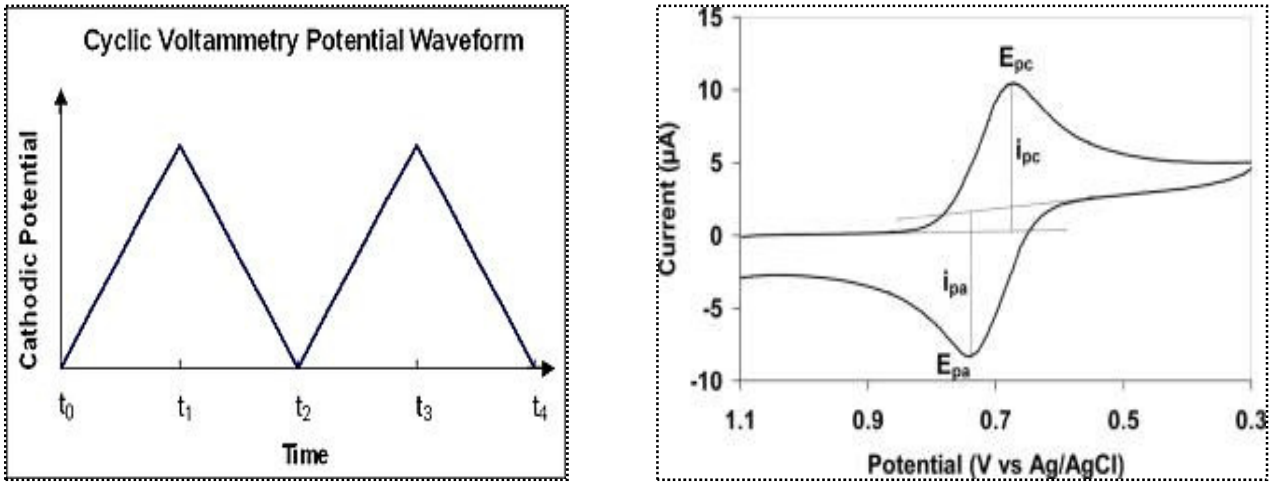

Figure: 1. (a) Excitation wave form of cyclic voltammetry (b) response obtained for the reversible cyclic voltammetry.

A cyclic voltammogram is obtained by measuring the current at the working electrode during the potential scan. The current measured can be considered as the response signal to the potential excitation signal. The voltammogram is a display of current (vertical axis) verses potential (horizontal axis). Because the potential varies linearly with time, the horizontal axis can also be thought as time axis [48-53].

Cyclic voltammetry has become an important and widely used electroanalytical technique in many areas of chemistry. It is rarely used for quantitative determinations, but it is widely used for the study of redox process, for understanding reaction intermediate, and obtaining stability of reaction products [48, 52, 53].

The important parameter of a cyclic voltammogram are the magnitude of the anodic peak current (I_{pa}), cathodic peak current (I_{pc}), anodic peak potential (E_{pa}) and cathodic peak potential (E_{pc}). A redox couple in which both species rapidly exchange electrons with the working electrode is termed as electrochemically reversible couple. Such couple can be identified from a cyclic voltammogram by measurement of the potential difference between the two peaks potential.

The formal reduction potential E^o, for reversible couple is centered between E_{pa} and E_{pc} [50, 52, 53]:

$$E^0 = \frac{E_{pa} + E_{pc}}{2}$$ ---------- (1)

The number of electrons transferred in the electrode reaction (n) for reversible couple can determined from the separation between peak potentials.

$$\Delta E = E_{pa} - E_{pc} \approx \frac{2.303RT}{nF}$$ ----------(2)

Where n is the number of electrons transferred and E_{pa} and E_{pc} are the anodic and cathodic peak potentials, respectively, in Volts. Thus for a reversible redox reaction at 25^{o}c with n electrons ΔE_p should be 0.0592/nV or about 60 mV for one electron.

Randles-Sevcik equation is an equation that correlates the peak current (I_p) with concentration (C), I_p = k C, where k is a constant that includes different cell parameters such as transfer coefficient, number of electrons involved in the reaction, electrode area, diffusion coefficient and scan rate [56].

$$I_p = 0.4463nFAC\left(\frac{nF\nu D}{RT}\right)^{1/2}$$ ----------(3)

n = number of electrons transferred

F = Faraday constant (96485.339 C/mol), A = the electrode surface area in (m^2), ν = scan rate in (Volt / s), R = gas constant (8.314J/K), T = Temperature (K) and C=concentration (mol/m^3)

2.2. **Pulse Methods**

The imposition of potential pulse to the electrode leads to in most experimental situations to a considerable improvement (increase) in the ratio of the charging and faradic currents compared to linear scan voltammetry. This is because the faradic current usually decreases with $1/t^{1/2}$ while

the charging current decreases much faster. In consequence, decreased lower limits of detection are obtained [55, 56].

2.2.1. Normal pulse voltammetry (NPV)

This technique uses a series of potential pulses of increasing amplitude (fig 2). The current measurement is made near the end of each pulse, which allows time for the charging current to decay. It is usually carried out in an unstirred solution at either DME (called normal pulse paleography) or solid electrodes. The potential is pulsed from an initial potential *Ei*. The duration of the pulse is usually 1 to 100 ms and the interval between pulses is typically 0.1 to 5 sec. The resulting voltammogram displays the sampled current on the vertical axis and the potential to which the pulse is stepped on the horizontal axis [54, 55].

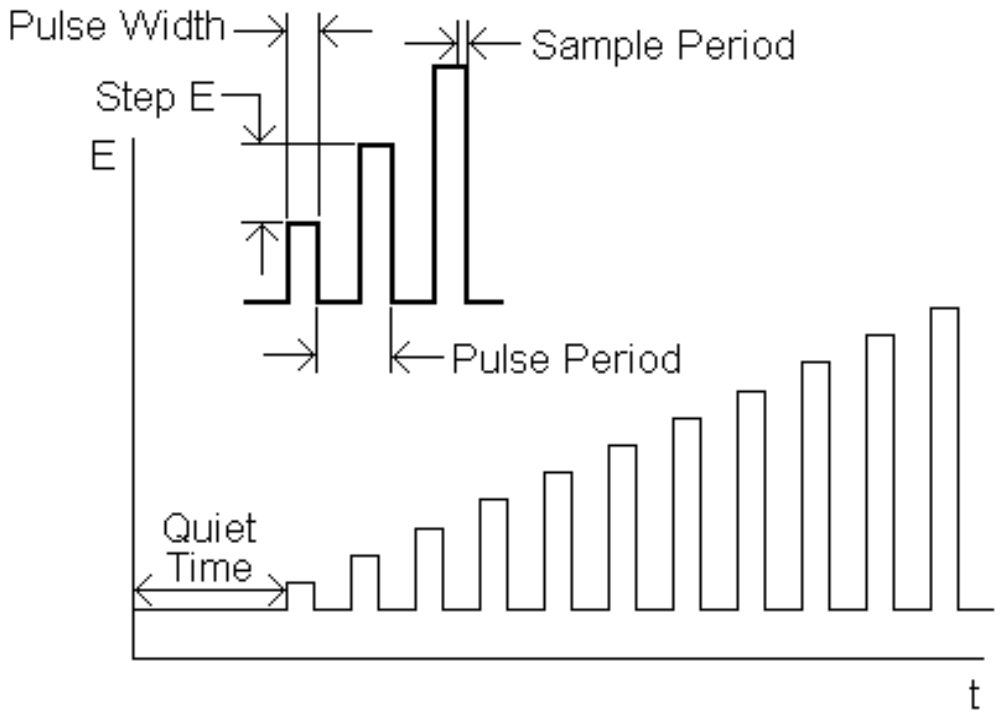

Fig.2. Excitation waveform of normal pulse voltammetry

2.2.2. Differential Pulse Voltammetry (DPV)

Differential pulse voltammetry can be considered as a series of regular voltage pulses superimposed on a linearly changing voltage, in which the resulting current is measured between the ramped baseline voltage and the pulse voltage. A digital staircase voltage is commonly used as the ramped baseline (Fig.3). This technique is comparable to normal pulse voltammetry in that the potential is also scanned with a series of pulses. However, it differs from NPV because each potential pulse is fixed, of small amplitude (10 to100 mV), and is superimposed on a slowly changing base potential. Current is measured at two points
for each pulse, the first point (1) just before the application of the pulse and the second (2) at the end of the pulse. These sampling points are selected to allow for the decay of the nonfaradic (charging) current. The difference between current measurements at these points for each pulse is determined and plotted against the base potential [56]. For reversible electrode reaction the peak current is given by:

$$I_p = \frac{nFAD^{1/2}C}{(\pi t_m)^{1/2}}\left(\frac{1-\sigma}{1+\sigma}\right) \quad \text{.....4}$$

where σ = exp [(nF/ RT)(ΔE/2)]. ΔE is the pulse amplitude.

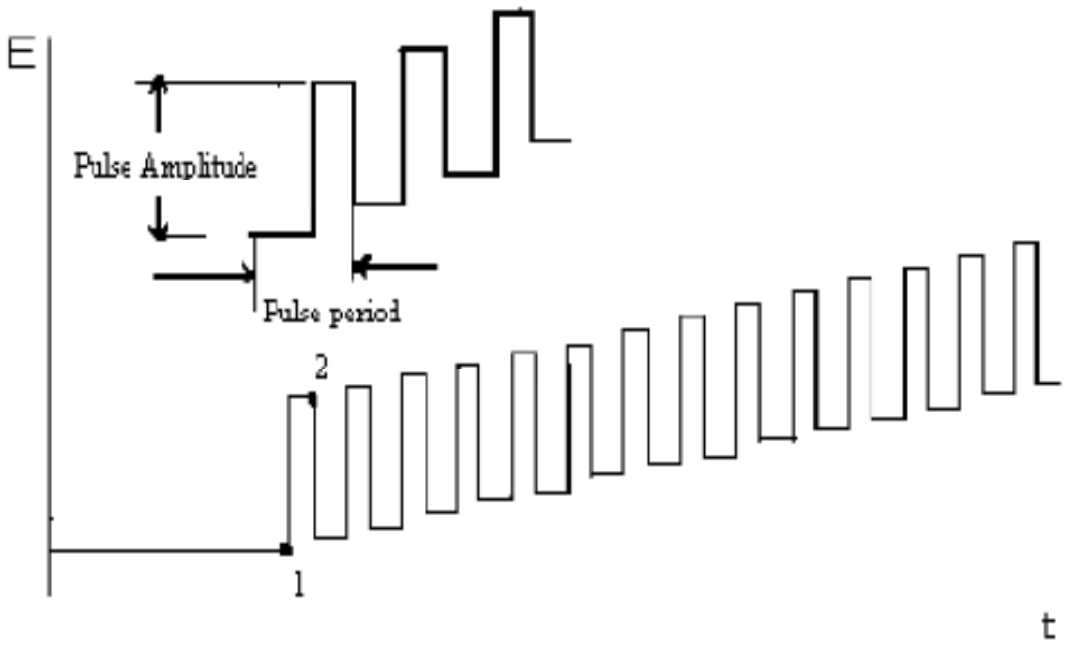

Fig .3. Excitation waveform of differential pulse voltammetry.

2.2.3. Square Wave Voltammetry (SWV)

Square wave voltammetry is a type of pulse voltammetry that offers the advantage of speed and high sensitivity. An entire voltammogram is obtained in a few seconds or less. The excitation signal in SWV consists of a symmetrical square-wave pulse of amplitude Esw superimposed on a staircase waveform of step height ΔEs, where the forward pulse of the square wave coincides with the staircase step (Fig.4). The net current, i_{net}, is obtained by taking the difference between the forward and reverse currents ($i_2 - i_1$) and is centered on the redox potential. The peak height is directly proportional to the concentration of the electroactive species. Excellent sensitivity is achieved from the fact that the net current is larger than either the forward or the reverse components, since it is the difference between them and detection limits as low as 1×10^{-8} M are possible [55].

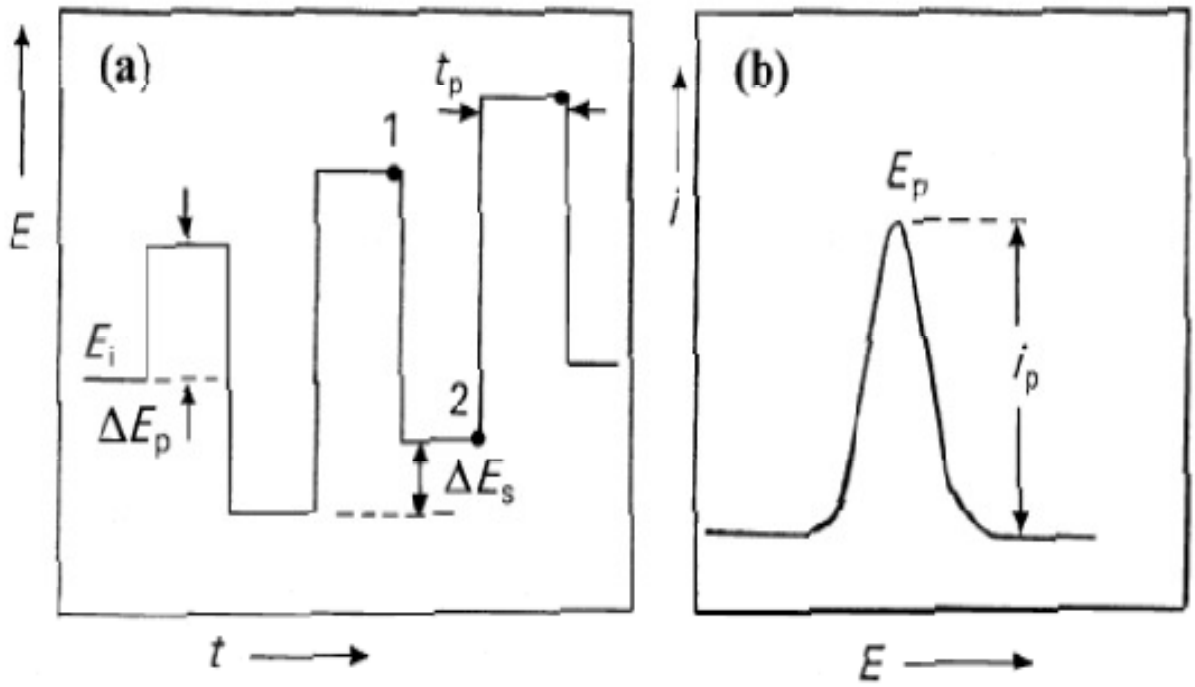

Fig (4). a. Excitation waveform of square wave voltammetry. b. Response obtained by square wave voltammetry.

Square-wave voltammetry has several advantages. Among these are its excellent sensitivity and the rejection of background current. Its speed, coupled with computer control and signal averaging, allows for experiments to be performed repetitively and increases the signal-to- noise ratio. The net peak current for the irreversible system is given by [54].

$$I_p = \alpha n^2 \Delta E E_{sw} (fD)^{1/2} C \quad \text{.....(5)}$$

where ΔE is the step potential, f is square wave frequency, E_{SW} is the square wave amplitude, α is the transfer coefficient, n is the over all electron transfer, C is the bulk concentration, and D is the diffusion coefficient of the electroactive species. The effective scan rate is given by fΔE. Kinetic parameters can also benefit from the rapid scanning and the reversal nature of square wave voltammetry. This method possesses both pulse and cyclic voltammetry; hence it is one of

the most advanced methods in the family of pulse technique.

Applications of square-wave voltammetry include the study of electrode kinetics with regard to preceding, following, or catalytic homogeneous chemical reactions, determination of some species at trace levels, and its use in electrochemical detection in HPLC [56].

OBJECTIVE:

1. To prepare Fe^{3+} doped-zeolite/graphite powder composite modified glassy carbon electrode.
2. To study the electroanalytical parameters of the modified electrode (linear range, sensitivity, detection limit, etc).
3. To study the analytical application of the Fe^{3+} doped-zeolite/graphite powder composite modified electrode for the determination of uric acid in human urine.

3. Experimental

3.1. Chemicals and Reagents

Ferric chloride (Research Chemicals Ltd, England), Zeolite Y, Hydrochloric acid (BDH, England), Polystyrene, Dichloroethane (Riedel-de Haen, Germany), Tetrahydrofuran (BDH, England), Uric acid (Research-lab Fine Chem Inustries, India), Graphite powder, Sodium nitrate (Riedel-de Haen, Germany), dipotassium hydrogen phosphate (Wagtech international Ltd, UK), Potassium dihydrogen phosphate (Riedel-deHaen, Germany).

Supporting electrolyte of phosphate buffers (KH_2PO_4 –K_2HPO_4) in the pH range 5-9 were prepared from 0.1 M KH_2PO_4 and 0.1 M K_2HPO_4 in distilled water. The pH of the solutions were adjusted by adding drops of concentrated H_3PO_4 and KOH. All experiments were carried out at room temperature and all solutions were prepared from deionized water.

3.2. Apparatus

All electrochemical measurements were performed with BAS-50W electrochemical analyzer. A conventional three–electrode system was employed with a bare GCE (3 mm in diameter), Fe^{3+} Y/GPC modified GCE, graphite powder modified GCE (GPMGCE), and non doped zeolite/GPC modified GCE as the working electrode, saturated calomel electrode (SCE) was used as the reference electrode and a platinum foil as the counter electrode. The pH of the buffer solution was measured with a Hanna digital pH 301 meter with combination glass electrode. All the potentials are determined with respect to a saturated calomel electrode as a reference electrode.

3.3. Electrode preparation

Four types of electrodes were used as working electrodes. These are bare GCE, GCE modified with graphite powder, GCE modified with undoped zeolite and graphite powder composite, GCE modified with Fe^{3+} doped-zeolite and graphite powder composite. The last three electrodes contain polished GCE, graphite powder, dichloroethane, tetrahydrofuran and polystyrene in common.

The iron (III) doped zeolite was prepared according to the previously described procedure [30]. Briefly, 1 g of zeolite was lightly ground and immersed in 250 mL of 0.01 M $FeCl_3$ solution and stirred for 48 h. The Fe^{3+} doped zeolite was carefully washed with HCl solution (pH of 2.0) to remove occluded material and surface-adherent salt, washed with distilled water to remove chloride ion, and finally dried at room temperature.

The iron (III) doped zeolite/ graphite powder composite modified GCE was prepared initially by lightly grinding a mixture of 50 mg of the iron (III) doped zeolite and an equal amount of graphite powder. Then the resulting composite was dispersed in a mixture of 0.2 mL of tetrahydrofuran, 0.3 mL of dichloroethane and 10 mg of polystyrene. The mixture was sonicated for 30 minutes after through hand - mixing. 10 µL of the mixture was casted on the surface of a well-polished GCE and dried at room temperature for about 30 minutes. The other modified electrodes were prepared following the same procedure but omitting the iron (III) exchanging

step or zeolite addition step. After this process, the modified electrode was immersed in pH 7.0 PBS until use.

For comparison, the responses of bare GCE, GCE modified with undoped zeolite/ Graphite powder composite, GCE modified with Iron (III) doped zeolite / Graphite powder composite and GCE modified with graphite powder for 1 mM uric acid in 0.5 mol L^{-1} $NaNO_3$ (pH 7.0 PBS) have been studied.

For the analytical performance of the method a series of concentration of uric acid ranging from 2 to 800 µM was prepared from a 1mM uric acid stock solution, which is prepared by weighing 16.8 mg of uric acid dissolving it with deionized water and diluting it to the mark to a100 mL volumetric flask with deionized water.

4. Results and discussion

4.1. Electrochemical characterization of Fe^{3+} Y/GPC modified GCE

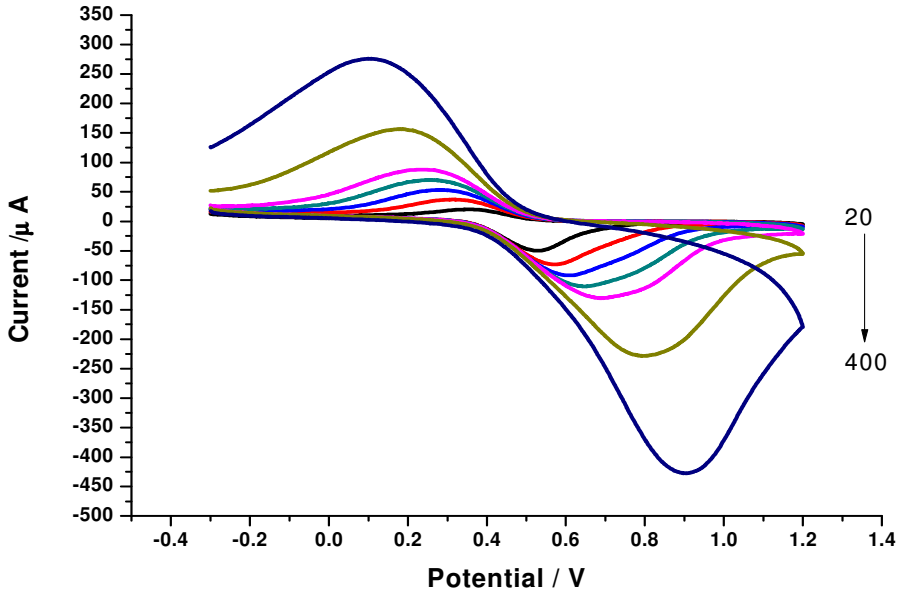

Fig. 5(A)

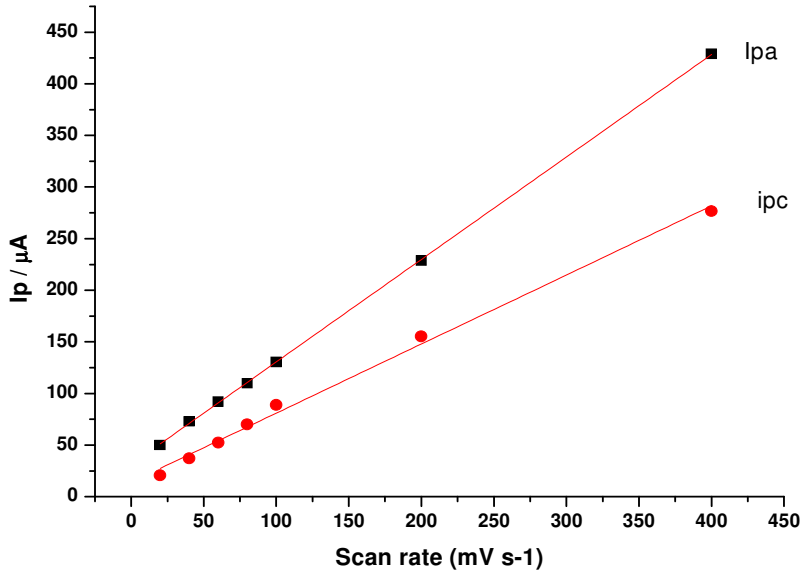

Fig. 5(B)

Fig. 5. (A) Cyclic voltammogram of stabilized Fe^{3+} Y/GPC modified GCE in 0.5 mol L^{-1} $NaNO_3$ (pH 7 PBS) at different scan rates (from inner to outer waves: 20,40,60, 80, 100, 200 and 400 mV s^{-1}). (B) Peak current (Ip) vs scan rate (ν).

Fig. 5A depicts the effect of potential scan rate on the CV of Fe^{3+} Y/GPC modified GCE in the 20 - 400 mV s^{-1} scan rate range. A pair of redox peaks was obtained characteristic of Fe^{3+}/Fe^{2+} indicating the incorporation of Fe^{3+} in to the cavities of zeolite. A linear relationship between oxidative and reductive peak currents with scan rates was found with linear equations and correlation coefficients as given below.

$$I_{pa}(\mu A) = 31.2375 + 0.99295\nu(mV\ s^{-1})\ (R^2 = 0.9999)\ \text{and}$$

$$I_{pc}(\mu A) = 13.99468 + 0.66934\nu(mV\ s^{-1})\ (R^2 = 0.9947)\ \text{respectively.}$$

This linear dependence of the peak current on the potential scan rate is an indication of redox processes for surface-confined species. Thus, we can conclude that the iron (III) is undergoing characteristic redox processes just on the surface of the electrode.

4.2. Electrochemical oxidation of uric acid at different electrodes

The responses of the modified electrodes for 1 mM UA in 0.5 mol L^{-1} $NaNO_3$ (pH 7.0 PBS) have been investigated.

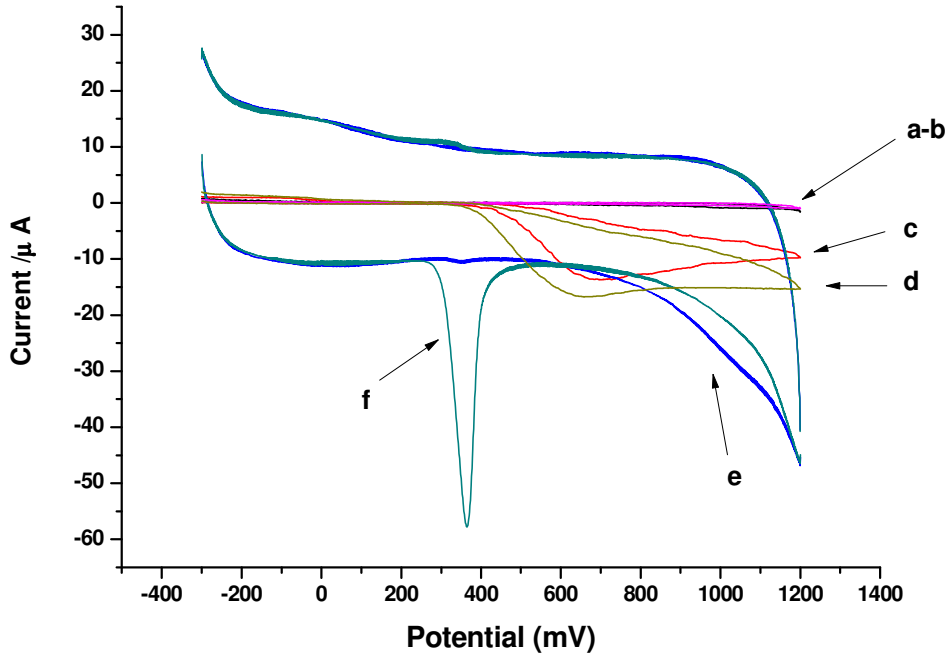

Fig. 6(A)

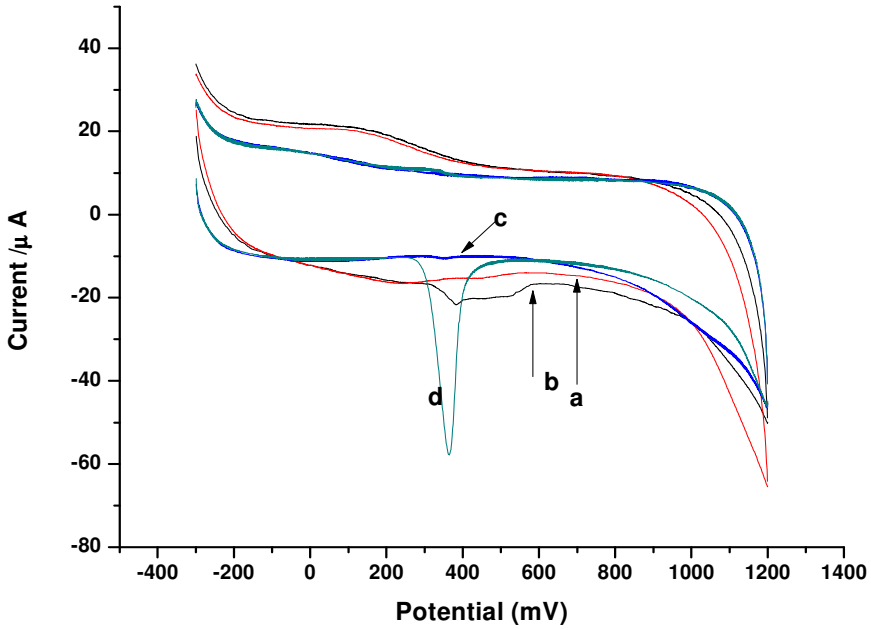

Fig. 6(B)

Fig.6. Cyclic voltammograms of (A) bare GCE (a and c), GPMGCE (b and d) and Fe^{3+} Y/GPC modified GCE (e and f) in 0.5 mol L^{-1} $NaNO_3$ (pH 7.0 PBS) containing no UA (a, b and e) and in 0.5 mol L^{-1} $NaNO_3$ (pH 7.0 PBS) containing 1 mM UA (c, d and f). (B) undoped zeolite/ GPC modified GCE (a and b) and Fe^{3+} Y/GPC modified GCE (c and d) in 0.5 M NaNO3 (pH 7.0 PBS) in the absence (a and c) presence (b and d) of 1 mM UA. Scan rate: 100 mV s^{-1}.

The cyclic voltammograms of 1 mM of UA in o.5 M $NaNO_3$ (pH 7.0 PBS) at different electrodes is shown in (Fig. 6). UA undergoes an irreversible oxidation at both the bare and graphite powder modified GCEs. The current response and peak potential of UA at the bare (Fig. 6A(c)) and graphite powder modified GCE (GPMGCE) (Fig. 6A(d)) are comparable. A fourfold increment of the peak current and a potential shift of about 300 mV to a lower positive potential (Fig. 6A(f)) have been observed at the Fe^{3+} Y/GPC modified GCE indicating the catalytic activity of the Fe^{3+} doped zeolite modified GCE which lowers the overpotential thereby facilitating the electron exchanging process between the analyte and the electrode surface.

Comparison has also been made between the current responses of the undoped and Fe^{3+} doped zeolite by recording their cyclic voltammograms (Fig. 6B) for 1 mM UA in 0.5 M $NaNO_3$ (pH

7.0 PBS). It can be concluded that the potential shift and current enhancement observed (Fig. 6A) is not due to the zeolite but due to the presence of the Fe^{3+} in the cavities of zeolite.

4.3. Effect of scan rate on the peak current and peak potential of UA at Fe^{3+} Y/GPC modified GCE

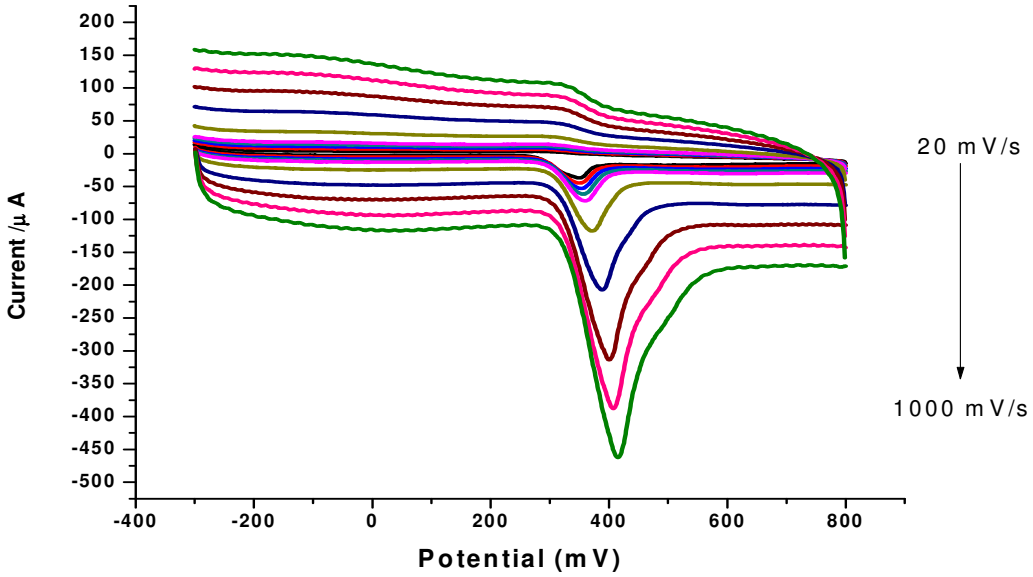

Fig. 7(A)

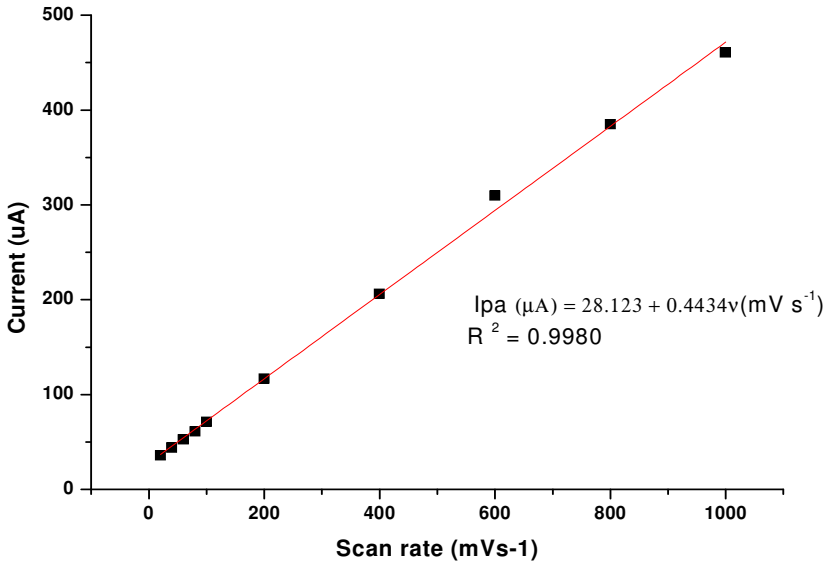

Fig. 7(B)

Fig.7. (A) Cyclic voltammograms of 1 mM UA in 0.5 M NaNO3 (pH 7.0 PBS) at different scan rates (20, 40, 60, 80, 100, 200, 400, 600, 800 and 1000 mV/s). (B) Plot of peak current versus potential scan rate.

The dependence of the peak current of UA on the potential sweep rate has been investigated. The oxidation current for 1 mM UA increased linearly with potential scan rate (ν) in the range 20 to 1000 mV s^{-1} (Fig. 7B) with a correlation coefficient of R^2 of 0.9980, suggesting that the reaction is electron transfer controlled. The peak potential shift to a more positive direction with increasing potential scan rate observed from Fig. 7A above is an affirmation for the irreversibility of the oxidation reaction of UA at the modified GCE.

4.4. Effect of the pH of the supporting electrolyte

The effect of the pH of the supporting electrolyte on the peak current and the peak potential for 1 mM UA at the Fe^{3+} Y/GPC modified GCE has been investigated. As seen in Fig. 8A both the peak current and peak potential varied with changes in the pH of the solution.

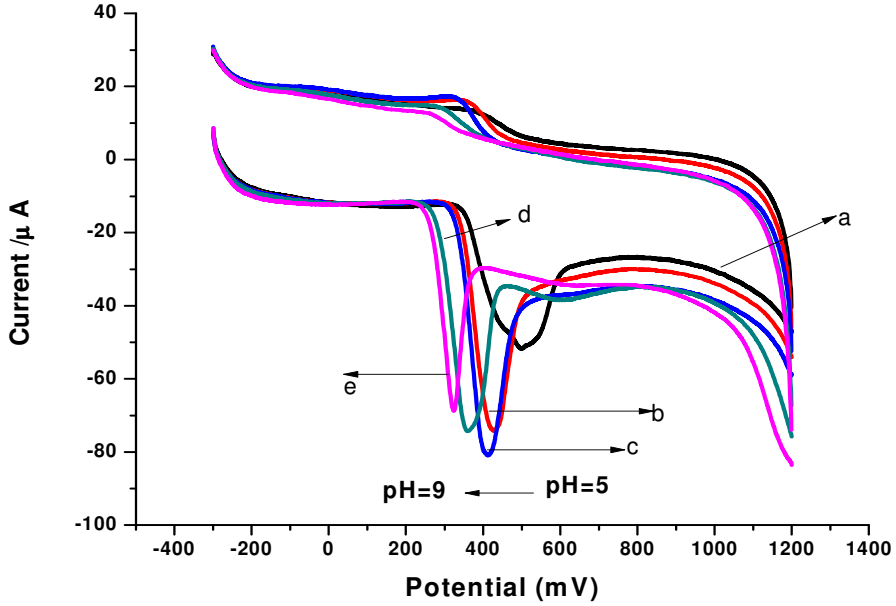
Current /µ A
Potential (mV)
a
b
c
d
e
pH=9
pH=5

Fig. 8(A)

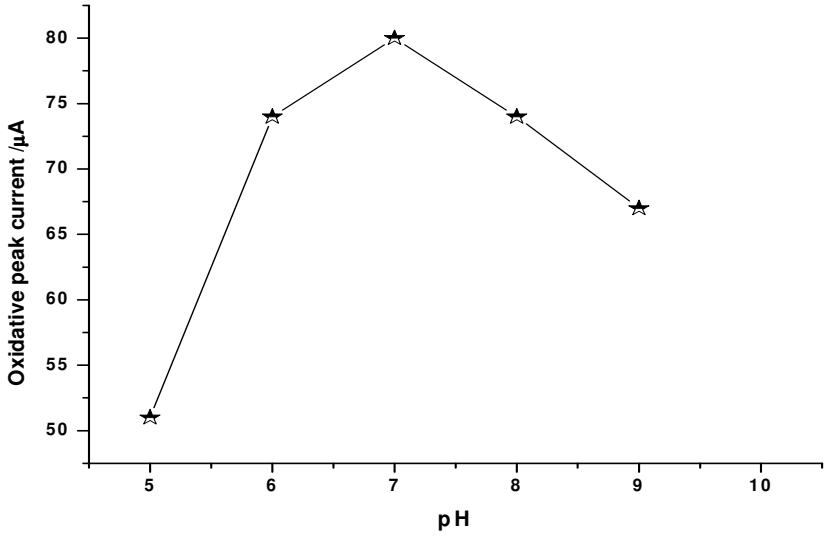
Oxidative peak current /µA
pH

Fig. 8(B)

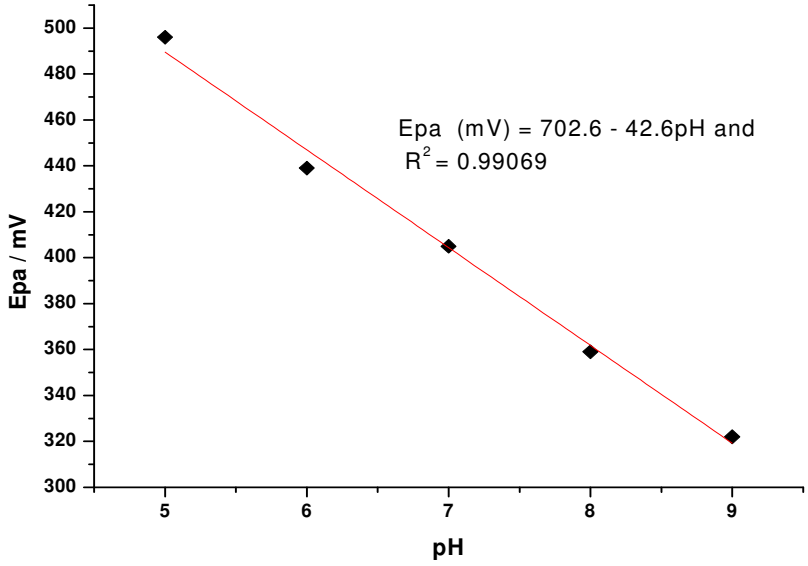

Fig. 8(C)

Fig.8. (A) Cyclic voltammograms of 1 mM UA in 0.5 M $NaNO_3$ (a to e): pH=5, pH=6, pH=7, pH=8, pH=9 at Fe^{3+} Y/GPC modified GCE, scan rate: 100 mV s^{-1}. (B) Dependence of the peak current for 1 mM UA on the pH of the supporting electrolyte. (C) Plot of peak potential versus the pH of the supporting electrolyte.

As can be seen from Fig. 8(B) the peak current increased dramatically with pH until it reached its maximum value at pH 7.0 which then decreased beyond pH 7.0. The trend could be explained taking two consequences of increasing the pH in to account. Firstly; with raising the pH of the solution, the uric acid (pKa = 5.8) becomes more negative and exerts stronger attractive force towards the Fe^{3+} doped zeolite surface of the GCE resulting an increase of the peak current with the pH. On the contrary, the extent the surface of the modified GCE is rich in the Fe^{3+} ions which catalyze the oxidation of UA gets lower. This is in agreement with the decreasing trend of the peak current with increasing the pH of solution above 7.0. Thus solution pH of 7.0 which is the physiological pH was taken the optimum pH.

The peak potential also showed linear shift to a more negative direction with increasing the pH of the supporting electrolyte from pH 5.0 to pH 9.0 with a regression equation and correlation coefficient of E_{pa} (mV) = 702.6 – 42.6pH and R^2 = 0.99069 respectively indicating the involvement of protons in the oxidation of UA. A slope of 42.6 mV is a confirmatory of equal number of electrons to the number of protons are involved in the oxidation of UA at Fe^{3+} Y

/GPC modified GCE [21]. Based on this findings, the most probable reaction mechanism for the oxidation of UA at Fe^{3+} Y/GPC modified GCE is shown below.

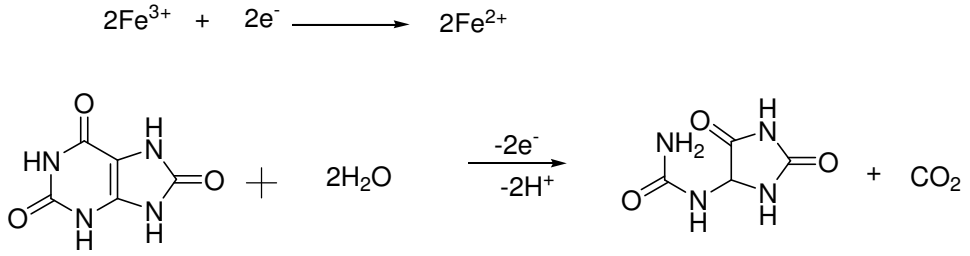

4.5. Square wave voltammetry of UA

The SW voltammograms of 1 mM UA in 0.5 M $NaNO_3$ (pH 7.0 PBS) at bare GCE and the iron (III) doped-zeolite graphite powder composite modified GCE are shown in Fig. 9. These voltammograms showed clearly the catalytic role of the modifier by lowering the over potential and facilitating the electron exchange process at the surface. Hence, square wave voltammetric method was used for the determination of UA concentration in real samples.

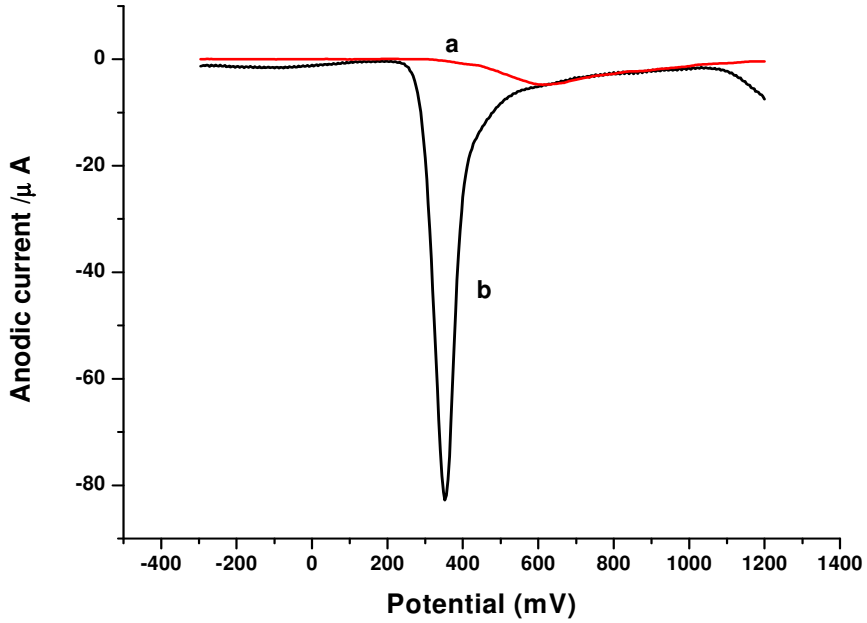

Fig.9. Square wave voltammograms of 1 mM UA in 0.5 M $NaNO_3$ (pH 7.0 PBS) at bare and Fe^{3+} Y/GPC modified GCE.

4.6. Influence of accumulation potential (E_{acc})

The effect of accumulation potential (E_{acc}) on the SWV peak current was studied at various accumulation potentials between -50 mV and 200 mV. The maximum peak current was obtained at an accumulation potential (E_{acc}) of +100 mV as shown in Fig. 10. Therefore the accumulation potential (E_{acc}) of +100 mV was chosen as the optimum potential.

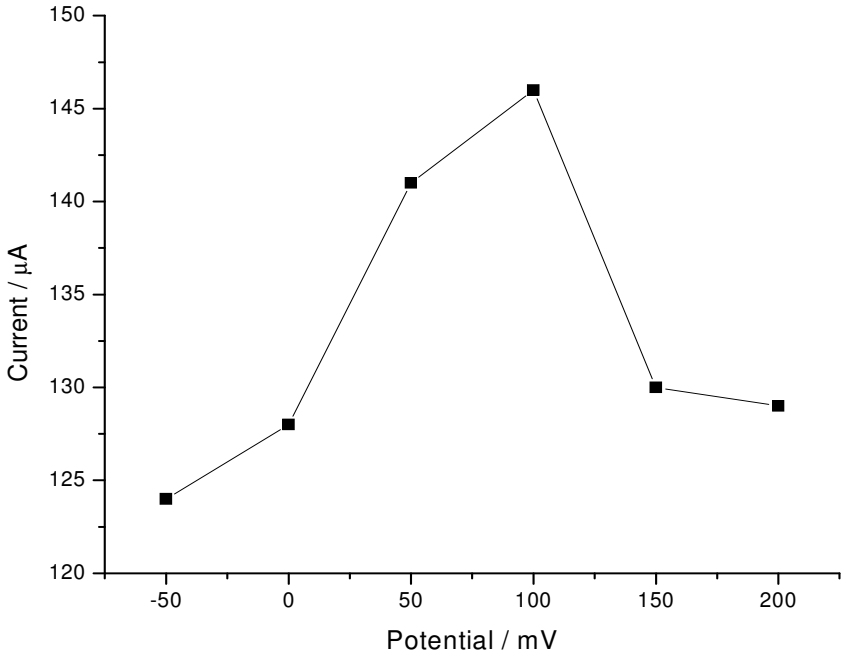

Fig.10. Effect of deposition potential on the SWV peak current for 1 mM UA in 0.5 M $NaNO_3$ (pH 7.0 PBS) at Fe^{3+} Y/GPC modified GCE. Amplitude: 20 mV; deposition time: 10 s.

4.7. Influence of accumulation time (t_{acc})

The effect of accumulation time (t_{acc}) on the peak current of UA was carried out using 1 mM UA. The responses obtained are shown in Fig. 11. The variation of adsorption time between 0 and 40 s at an adsorption potential of 100 mV, showed that the peak current increased with the increase in accumulation time (t_{acc}) up to 30 s and then leveled off.

The increase of peak current with increase in accumulation time (t_{acc}) indicated that UA can be accumulated at the zeolite cavities on the surface of the GCE. The leveling off in peak current after 30 s shows the saturation of the cavities. So the accumulation time of 30 s was selected as an optimum accumulation time (t_{acc}) for further experiments.

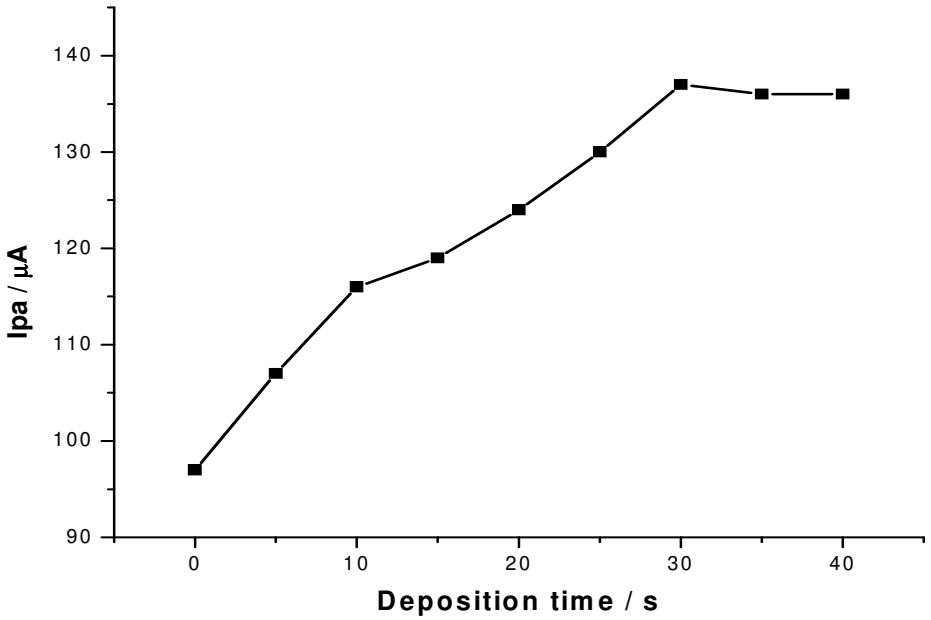

Fig.11. Effect of deposition time on the oxidative peak current of 1 mM UA in 0.5 M $NaNO_3$ (pH 7.0 PBS). Deposition potential: 100 mV

4.8. Analytical performance of the method

The optimum conditions selected for the determination of uric acid using square wave voltammetry were: pulse amplitude 40 mV, Scan rate100 mV/s, accumulation time 30 s, and accumulation potential +100 mV. Under these optimum conditions, the oxidation peak current of UA increased linearly with concentration in the range of 2.0×10^{-6} to 8.0×10^{-5} mol L^{-1} with linear equation, correlation coefficient (R^2) and detection limit (based on the formula LoD = 3δ/m) of I_{pa} (μA) = 0.1952 – 0.3252C (μM), 0.99903 and 2.32 x 10^{-7} mol L^{-1} respectively.

.

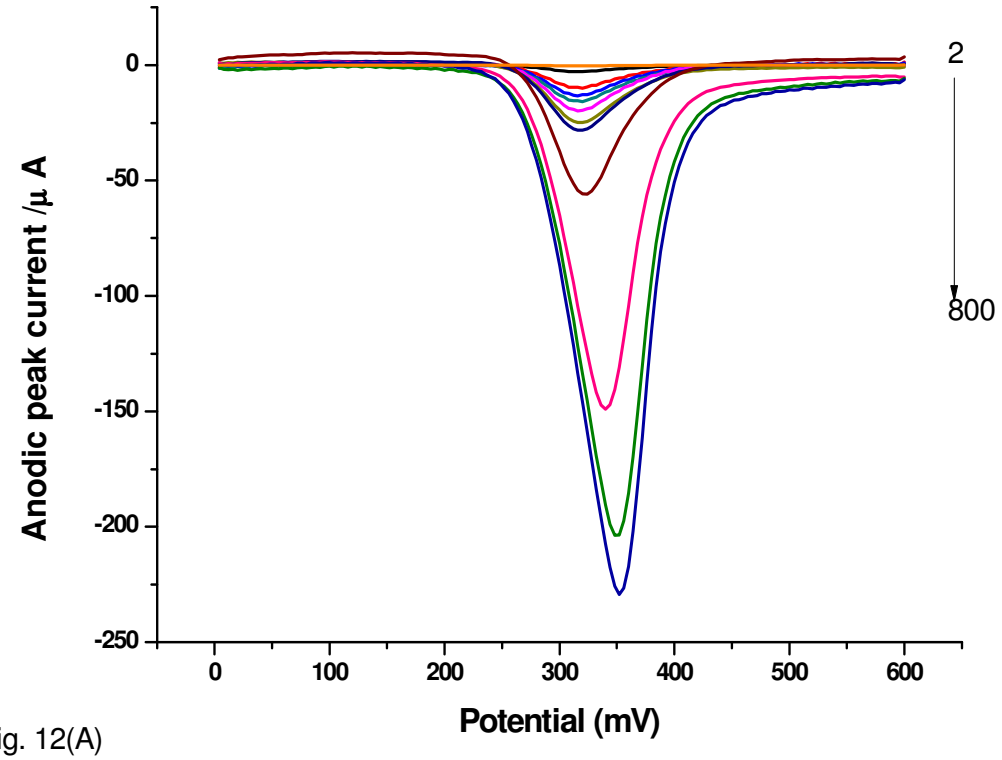

Fig. 12(A)

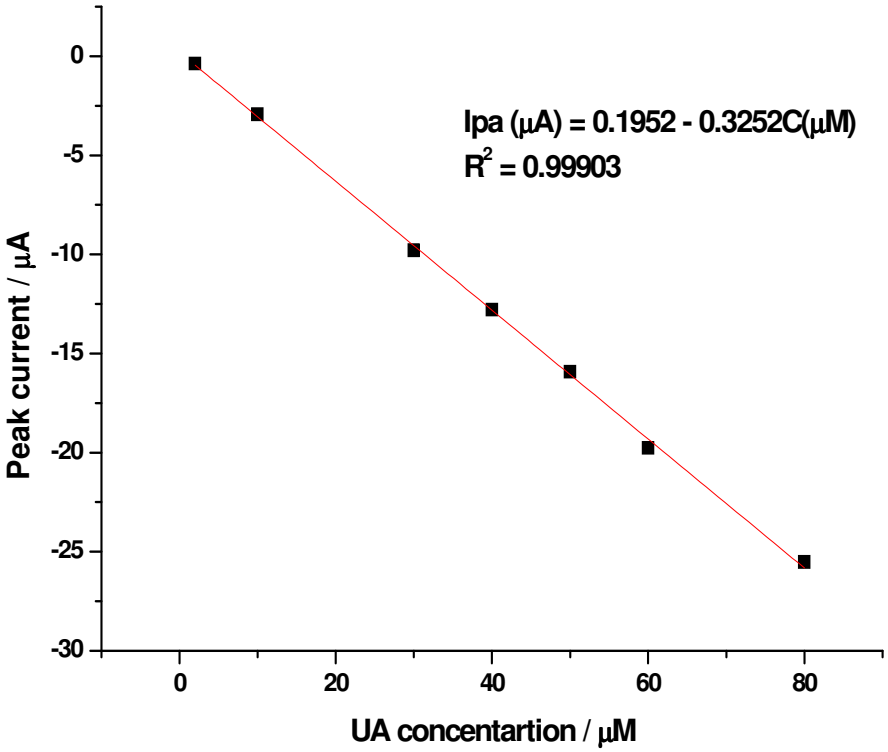

Fig. 12(B)

Fig.12.(A) Square wave voltammograms of Fe^{3+} Y/GPC modified GCE for different concentrations (2, 10, 30, 40, 50, 60, 80, 100, 200, 400, 600 and 800μM) of UA in 0.5 M $NaNO_3$ (in pH 7.0 PBS) at scan rate, deposition time, deposition potential and pulse amplitude of 100 mV s^{-1}, 30 s, 100 mV and 40 mV (B) Plot of peak current versus concentration.

Table1. Comparison of the proposed electrode with other modified electrodes

Electrode	Modifier	LR($molL^{-1}$)[a]	LOD($molL^{-1}$)[b]	References
Carbon paste electrode	Fe^{3+}doped zeolite	0.3-700 µ	0.8×10^{-7}	22
Glassy carbon electrode	Carbon-coated nanoparticle	0.5-20 µ	1.5×10^{-7}	21
Carbon paste electrode	Nafion	0-50 µ	2.5×10^{-7}	17
Glassy carbon electrode	Poly(N,N-dimethylaniline)	1.25-68.75 µ	1.25×10^{-6}	18
Glassy carbon electrode	Cysteine	0.7-300 µ	3.7×10^{-7}	20
Glassy carbon electrode	Poly(bromocresol purple)	0.5-120 µ	2×10^{-7}	23
Glassy carbon electrode	Fe^{3+}doped zeolite/graphite	2-80 µ	2.32×10^{-7}	This work

[a]Linear range

[b]Limit of detection

4.9. Analytical applications

In order to evaluate the validity of the proposed method, the Fe^{3+} doped zeolite/graphite powder composite modified GCE was applied for the direct determination of uric acid in urine samples collected from three different volunteers. The method was also used to determine concentrations of standard uric acid spiked in to urine solutions. The collected urine samples were divided in to two portions; one portion for analysis after suction filtration with 0.45 µm filter paper and the other portion for direct analysis without filtration.

To fit into the linear range, all the human urine samples (filtered and unfiltered) were diluted 200 times [17] with 0.5 M $NaNO_3$ (pH 7.0 PBS) to reduce the matrix effect of the human urine samples. Thus, determination of the UA from three human urine samples were performed with the diluted samples while recovery analysis of the standards (30, 50 and 70 µM) were from solutions of the standard UA and the diluted human urine samples. To determine the accuracy of

the results, three measurements have been carried for each sample. The results obtained are given in Table 2.

Table 2

Direct determination of UA in three filtered and unfiltered diluted human urine samples.

Urine sample code	Unfiltered urine			Filtered		
	Ipa* (µA)	Conc. (µM)	Standard deviation	Ipa* (µA)	Conc. (µM)	Standard deviation
1	2.420	8.0418	0.305	1.817	6.1866	0.193
2	4.987	15.935	0.021	4.723	15.124	0.123
3	6.960	22.002	0.546	6.517	20.640	0.280

* Mean anodic peak current of Triplicate measurements

As can be seen from Table 2, the detected concentrations of uric acid in the three unfiltered and filtered human urine samples are all in the uric acid concentration range for a normal person which is 1.5 – 4.5 mM [1] with standard deviations less than unity. The lower concentration of UA in the filtrated sample labeled code 1 could be ascribed to the possible mass loss during the filtration in the raw urine. The similarity between the responses for the UA concentrations detected in the filtrated and unfiltrated urine sample showed the selectivity of the developed method. These results suggested the modified electrode for the direct determination of UA in human urine without any treatment as in most of the conventional techniques.

Compared to the official method of determining uric acid, the proposed modified electrode does not need prior treatment of sample.

Table 3
Recovery of standard UA from three filtered and unfiltered human urine samples.

Urine sample	Unfiltered urine sample					Filtered urine sample				
	UA			SD**	% Recovery	UA			SD**	% Recovery
	present* (μM)	added (μM)	found (μM)			present* (μM)	added (μM)	Found (μM)		
1	8.0418	30.0	38.198	0.500	100.52	6.1866	30.0	38.218	0.210	106.77
		50.0	53.532	0.480	90.98		50.0	53.665	0.707	94.96
		70.0	75..990	0.414	97.07		70.0	72.033	0.916	94.07
2	15.935	30.0	44.276	0.534	94.47	15.124	30.0	45.362	0.430	100.79
		50.0	64.356	0.386	96.84		50.0	63.515	0.340	96.78
		70.0	82.724	0.448	95.41		70.0	81.904	0.207	95.40
3	22.002	30.0	50.416	0.282	94.71	20.640	30.0	50.723	0.295	100.28
		50.0	68.979	0.140	93.95		50.0	69.624	0.889	97.97
		70.0	86.506	0.668	92.15		70.0	87.716	0.210	95.82

* mean concentration of UA detected in the 200 times diluted human urine as per the results in table 1.
** Standard deviation of triplicate measurements.

The developed method was applied for the determination of uric acid spiked with human urine. The determination results and recoveries are listed in Table 3. It can be seen that recovery varied from 90.98% to 106.77%, indicating that the method developed is suitable for determination of uric acid in human urine. The system exhibited excellent reproducibility, with relative standard deviation less than 0.3. This makes it suitable for routine analysis.

5. Conclusion

In the present work, we introduced a new electrode based on iron (III) doped zeolite graphite powder composite modified glassy carbon electrode. Iron (III) loaded in zeolite matrix can increase anodic peak current by adsorption of uric acid compound on the electrode surface. The results indicated that Fe^{3+} Y/GPC modified GCE facilitate the determination of uric acid with good sensitivity and reproducibility. The proposed electrode was used in determination of uric acid in human urine with out the necessity for sample pretreatment or any time consuming

extraction steps prior to the analysis, with satisfactory recovery. The simple fabrication procedure, reproducibility, wide linear dynamic range, low detection limit, high sensitivity, suggests that this electrode is suitable for routine analysis.

6. REFERENCES

1. R. T. Kachoosangi, C.E. Banks, R.G. Compton, Electroanalysis, 2006, **18**, 741-747.
2. J.I. Yamakita, T. Yamamoto, Y. Moriwaki, Z. Tsutsumi, Ann Clin Biochem, 2000, **37**, 355-359.
3. J. M. Zen, P. J. Chen, Anal. Chem.,1997, **69**, 5087.
4. S. I. I. T. Nakaminami, S. Kuwabata, H. Yoneyama, Anal.Chem., 1999, **71**, 1928.
5. R. Bravo, C. C. Hsueh, A. Jaramillo, A. Brajter-Toth, Analyst, 1998, **123**, 1625
6. L. Fernandez, H. Carrero, Electrochimica Acta, 2005, 50, 1233-1240.
7. M. A. Ross, J. Chromat. B,1994, **657**, 197.
8. A. P. Louisi, S. Pascalidou, Anal. Biochem., 1998, **263**, 176.
9. J. Lykkesfeldt, Anal. Biochem., 2000, **282**, 89.
10. K. Safranow, Z. Machoy, J. Chromat. B, 2005, **819**, 229.
11. S.K. George, M.T. Dipu, U.R. Mehra, P. Sing, J. Chromat. B., 2006, **832**, 134-137.
12. H. L. Lee, S. C. Chen, Talanta, 2004, **64**, 750.
13. Y. Guan, T. Wu, J. Ye, J. Chromat. B., 2005, **821**, 229.
14. J. PerellPo, P. Sanchis, F. Grases, J. Chromat. B., 2005, **824**, 175.
15. B. A. Dilena, M. J. Peake, H. L. Pardue, J.W. Skorg, Clin. Chim. Acta.,1986, **32**, 486.
16. J. V. Pilleggi, J. D. Giorgio, R. D. Wybenga, Clin. Chim. Acta., 1972, **37**, 141.
17. J.M. Zen, C.T. Hsu, Talanta, 1998, **46**, 1363.
18. P.R. Roy, T. Okajima, T. Ohsaka, J. Electroanal Chem., 2004, **561**, 75-82
19. Quanping Yan, Faqiong Zhao, Guangzu Li, Baizhao Zeng, Electroanalysis,2006, **11**,1075
20. Zhu Yan, J.R. Zhang, H.Q. Fang, Analytical letters,1999, **32**, 223.
21. Shengfu Wang, Qiao Xu, Guodong Liu, Electroanalysis, 2008, **20**, 1116
22. Ali Babaei, M. Zendehdel, B. Khalizadeh, A. Taheri, Colloids and Surfaces B: Biointerfaces., 2008, **226**
23. Yan Wang, Li-li Tong, Sensors and Actuators B, 2010, **150**, 43
24. D.R. Rolison, Chem. Rev.,1990, **90**, 867.
25. A. Walcarius, Analytica Chimica Acta., 1999, **384**, 1-16
26. C.E. Marshall. J Phys Chem, 1939, **43**, 1155-1164

27. R.M. Barrer, S.D. James, J Phys Chem, 1960, **64**, 417-427
28. D.C. Freeman , Us Patent Number 3, 186,875 (1965),Br Patent No. 999,948 (1965).
29. N. Petranovic, M.V. Susic, Zeolites 3:271-273, 1983
30. J. P. Pereira-Ramos, R. Messina, J Perichon, J Electroanal Chem.,1983, **146**, 157-169.
31. C.G. Murry, RJ Nowak, D.R. Rolison, J Electroanal Chem., 1984, **164**, 205-210.
32. B. de Vismes, F. Bedioui, J. Devynck, C. Bied-Charreton, J Electroanal Chem.,1985,**187**, 197-202.
33. P. Hernandez, E. Alda, L. Hernandez, Fresenius, J Anal Chem., 1987, **327**, 676-678.
34. H.A. Gemborys, B.R. Shaw, J Electroanal Chem., 1986, **208**, 95-107.
35. S. Mintova, V. Valtchev, V. Engstrom, B.J. Schoeman, J. Sterte, Micropor Mater., 1997, **11**,149-160.
36. J. Coetzer, Electrochim Acta., 1978, **23**, 787-789.
37. M.D. Baker, C. Senaratne, Anal Chem., 1992, **64**, 697-700.
38. R.N. Adams, Electrochemistry at Solid Electrodes, New York: Marcel Dekker, 1969
39. K. Kalcher, J.M. Kauffmann, J. Wang, I. Svancara, K. Vytras, C. Neuhold, Z. Yang, Electroanlysis, 1995, **7**, 5-22.
40. A. Walcarius, T. Barbaise, J. Bessiere, Anal Chim Acta., 1997, **340**, 61-76.
41. B.R. Shaw, K.E. Creasy, C.J. Lanczycki, J.A. Sargeant, M. Tirhado, J Electrochem Soc., 1988, **135**, 869-876
42. P.K. Dutta, M. Ledney, Progr Inorg Chem., 1997, **44**, 209-271
43. C.A. Bessel, D.R. Rolison, J. Phys Chem., 1997, **101**, 1148-1157
44. M.D. Baker, C. Senaratne, J. Zhang, J. Chem Soc Faraday Trans., 1992, **88**, 3187-3192
45. J. Li, K. Pfanner, G. Calzaferri, J. Phys Chem., 1995, **99,** 2119- 2126
46. Z. Li, T.E. Mallouk, J. Phys Chem., 1987, **91**, 643-648
47. F. Bedioui, J. Devynck, K.J. Balkus, J. Phys Chem., 1996, **100**, 8607-8609.
48. P. Proti, Introduction to Modern voltammetric and polarographic Analysis Techniques, Amel electrochemistry,4th edition., New York,**2001**.
49. S.P. Kounaves, Hand book of Instrumental techniques for analytical chemistry, John Willey and Sons,Inc., chapter 37,New York,711.

50. W.R. Lacourse, Pulsed electrochemical detection in HPLC, John Willey and Sons, Inc., New York, **1997**,47-48.
51. D.T. Sawyer, W.R. Heimeman, and J.M. Beebe, Chemical experiments for instrumental methods, John willey and sons., New York, **1984**, 80-85.
52. L.L. Merrit, J.A. Dean, F. Sttle, and Willard, Instrumental methods of analysis, Litton educational puplishing,Inc., 6th edition., New York, **1981**,712-713.
53. P.T. Kissinger, and W.R. Heinemann, Laboratory techniques in electro analytical chemistry ,Marrcel Dekker,Inc., New York, 2nd edition, **1996.**
54. A.J. Bard, L.R. Faulkner, *Electrochemical Methods*: Fundamental and Applications, 2nd ed., John Wiley, New York, **2001.**
55. F. Scholz (Ed), Electro analytical Methods Guide to Experiments and applications springer, **2005**.
56. D. A. Skoog, D. M. West, and F. J. Holler, Fundamentals of Analytical chemistry, 7th Edition, Harcourt, **1996.**